Alloy Design Strategies for Promoting Protective Oxide-Scale Formation

M.P. Brady, B. Gleeson, and I.G. Wright

Editor's Note: Compositions are given in weight percent unless otherwise noted.

This article discusses general strategies for designing alloys to form protective oxide scales. Approaches based on classical alloy-oxidation theories work reasonably well for single-phase alloys. However, high-temperature alloy development has been and will increasingly be based on multiphase microstructures in order to achieve many of the needed, but usually opposing properties, such as high-temperature strength and room-temperature toughness. No theoretical-based, well-defined strategies exist for the design of oxidation-resistant multiphase alloys. Still, key factors are beginning to emerge, which can provide guidance for promoting the formation of protective scales on multiphase alloys and for taking advantage of some unique mechanisms that are operative in multiphase alloys but not in single-phase alloys.

INTRODUCTION

Most high-temperature environments of technological interest contain sufficient reactive gaseous species that nearly all metals are thermodynamically unstable and convert to oxides, nitrides, carbides, sulfides, chlorides, etc. Such conversion processes are generically termed oxidation. The rate of oxidation depends primarily on the specific characteristics of the reaction product formed, which is determined by a complex interplay among composition, microstructure, and surface condition of the alloy with the thermochemistry of the environment and the temperature of the reaction. Oxidation can lead to a loss of load-bearing capacity in a component by the reduction of metallic cross section and, for many high-temperature applications, is the primary factor limiting service life. Interstitial dissolution of oxygen, nitrogen, etc. into an alloy during elevated-temperature exposure, which may accompany oxidation, can also degrade mechanical properties and result in component failure.

In practice, the oxidation of metals in many applications is not prevented, rather it is managed. Protection of the underlying metal is most often accomplished by the formation of a continuous scale over the surface such that it serves as a barrier between the remaining underlying, unoxidized metal and the environment. Long-term protection is generally associated with a scale that grows by a diffusion-controlled process or processes because the rate of scale growth slows with reaction time as the diffusion distance (scale thickness) increases. Most high-temperature environments of technological interest contain at least some oxygen. Given the fact that metal oxides are nearly always more stable thermodynamically than the corresponding metal nitrides, carbides, sulfides, chlorides, etc., the formation of an oxide scale is the preferred protection mode.

PROTECTIVE OXIDE-SCALE FORMATION

What constitutes a protective oxide scale depends on the desired lifetime of the component and the expected service conditions. For long-term (>>1,000 hours) use above about 600°C, Cr_2O_3, Al_2O_3 (α), and SiO_2 are the principal oxides used for protection. These oxides offer the potential for protection because the rates of metal and oxygen diffusion in the oxides are sufficiently low that they grow (oxidize) at an acceptably slow rate. In general, for long-term service under isothermal conditions, Cr_2O_3 scales can provide protection up to a maximum of around 1,000–1,100°C; Al_2O_3 to around 1,400°C; and SiO_2 to around 1,700°C. A complicating factor for both Cr_2O_3 and SiO_2 scales is volatility, especially in the presence of water vapor and/or in environments where there is flow, which can significantly (greater than several hundred degrees) reduce the maximum-use temperature.[1,2]

There are two key factors for protective oxide-scale formation: thermodynamic stability and protective oxide con-

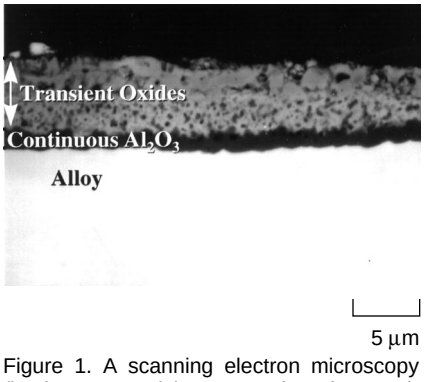

Figure 1. A scanning electron microscopy (backscatter mode) cross-section micrograph of Nb-33Ti-40Al (in at.%) after 15 minutes at 1,400°C in air. The continuous Al_2O_3 scale cuts off the formation of more rapidly growing niobium-rich transient oxides.[3]

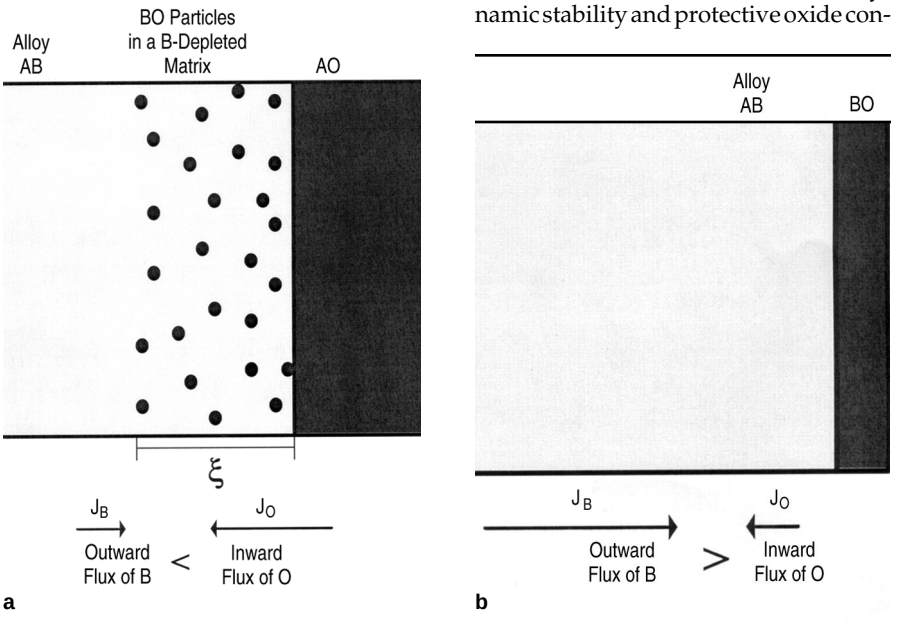

Figure 2. A schematic of (a) internal BO formation beneath a rapidly growing AO scale; and (b) external protective BO scale formation. Note that BO is thermodynamically more stable than AO.

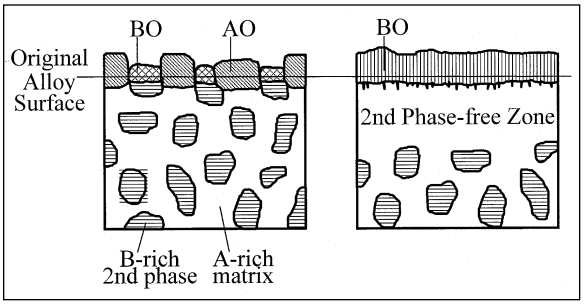

a b

Figure 3. A schematic showing (a) two phases oxidizing independently to form a nonuniform, nonprotective AO + BO scale, and (b) dissolution of a B-rich second phase in support of protective BO scale formation.[41]

tinuity. During the initial or transient stage of oxidation, nuclei of virtually all thermodynamically stable oxides of the alloy components form, including rapidly oxidizing elements. In order to achieve protective oxidation behavior, Cr_2O_3, Al_2O_3, or SiO_2 must be the most thermodynamically stable oxide of all of the major base alloy components. Under this constraint, if a continuous layer of the protective oxide can be established, the oxygen potential (i.e., partial pressure) at the alloy/scale interface is reduced below that at which the less-protective oxides are stable. Steady-state selective oxidation governed by Cr_2O_3, Al_2O_3, or SiO_2 formation then ensues. An example of this is shown in Figure 1, where the formation of a continuous Al_2O_3 layer locally cut off the growth of fast-growing, transient niobium-rich oxides during oxidation of a Nb-Ti-Al alloy at 1,400°C in air.[3]

It is important to note that maintaining protective oxide-scale formation is often not a trivial matter. Of particular concern is loss of oxide-scale adherence, especially under thermal cycling conditions. Due to subsurface compositional changes in the alloy, which may result from the selective consumption of chromium, aluminum, or silicon, the ability of the alloy to reform a protective Cr_2O_3, Al_2O_3, or SiO_2 scale after spallation may be compromised or lost. Issues relating to maintaining adhesion of oxide scales are addressed in the article by Smialek in this issue of *JOM*.[4]

OXIDATION OF SINGLE-PHASE ALLOYS

The thermodynamic and kinetic aspects of single-phase alloy oxidation have been extensively studied and reviewed (e.g., References 5–9). The basic parameters that dictate the formation of a protective scale are fairly well established, and, for binary and ternary alloys, the critical concentrations of chromium, aluminum, or silicon additions needed to form and maintain a protective oxide can be reasonably approximated if sufficient input data are available.

Compositional and Kinetic Factors Affecting Protective-Scale Formation

Figure 2 shows schematic diagrams of two limiting cases resulting from the oxidation of a binary alloy AB for which AO, a rapidly growing, nonprotective oxide, is less stable than BO, a protective oxide, such as Cr_2O_3, Al_2O_3, or SiO_2. AO and BO are assumed to be mutually insoluble and the oxygen partial pressure in the atmosphere is sufficiently high for both oxides to be stable. The two limiting cases shown are the formation of internal BO particles within the alloy and beneath the AO scale (Figure 2a) and the exclusive formation of a continuous, protective scale layer of BO (Figure 2b). These cases are most applicable to the situation where the difference in thermodynamic stability between AO and BO is large.[10]

Internal oxidation usually proceeds according to a parabolic rate law expressed in the form[11]

$$\xi^2 = 4\gamma^2 D_O t \qquad (1)$$

where ξ is the thickness of the internal oxidation zone at time t, D_O is the diffusion coefficient of oxygen in the alloy, and γ is a dimensionless kinetics parameter. The value of γ is inversely related to the atomic concentration of B in the bulk alloy, N_B^o, and the interdiffusion coefficient in the alloy, D_{AB}, but it is directly related to the solubility of oxygen at the alloy surface, N_O^s. Therefore, ξ tends to decrease with increasing N_B^o and decreasing permeability of oxygen in the alloy ($N_O^s D_O$). Departures from predicted classical behavior have been observed, particularly when the internal oxides are accicular and oriented perpendicular to the alloy surface (e.g., Al_2O_3 in the Ni-Al system).[12] In such cases, the kinetic expression must be modified to account for the enhanced diffusion of oxygen along the interfaces between the alloy matrix and the internal oxide.[13] Notwithstanding, ternary and higher-order alloying additions which effectively increase N_B^o or decrease N_O^s are beneficial in reducing ξ (e.g., References 14 and 15).

The transition from internal to external BO formation requires that a critical concentration of B in the bulk alloy, N_B^o*, be exceeded. The value of N_B^o* is dependent on kinetic rather than thermodynamic factors, although clearly the alloy must contain a sufficient concentration of B to maintain BO stability at the BO/alloy interface during steady-state growth. This "thermodynamically required" concentration is usually quite small for the highly stable oxides Cr_2O_3, Al_2O_3, and SiO_2,[10,16] and is significantly below the critical concentration required by kinetic considerations.

The treatments to predict N_B^o* (e.g., References 17 and 18) are based on the

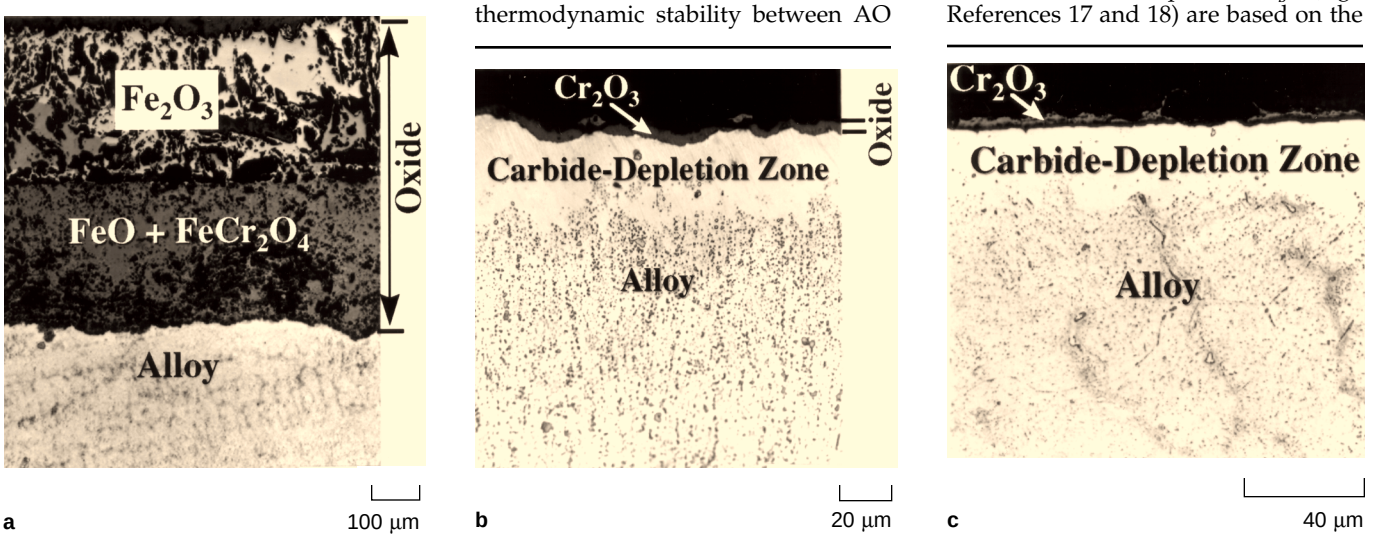

a b c

Figure 4. Optical cross-section micrographs of (a) as-cast Fe-15Cr-0.5C at 850°C, 72 hours, 1 atm oxygen; (b) hot-forged Fe-15Cr-0.5C at 850°C, 72 hours, 1 atm oxygen; and (c) as-cast Fe-14Cr-0.4C-1Si-1Ni at 850°C, 14 days, 1 atm oxygen.[50]

assumption that the volume fraction of BO in the internal oxidation zone, f_v, increases with increasing B concentration to the extent that oxygen diffusion in the alloy becomes so restricted that external BO formation is favored. The critical value of f_v is usually taken to be 0.3, reported originally by Rapp[19] from his study of the oxidation of Ag-In alloys at 550°C. It is approximately found that

$$N_B^o{}^* \approx \tfrac{1}{2}\gamma\phi^{1/2}\exp(\gamma^2\phi)\mathrm{erfc}(\gamma\phi^{1/2}) \quad (2)$$

where $\phi = D_O/D_{AB}$, γ is the kinetics parameter appearing in Equation 1, and erfc(z) is the complementary error function of z. It can be inferred from Equation 2 that $N_B^o{}^*$ decreases with $\gamma\phi^{1/2}$. Thus, external BO formation is favored by a high value of D_{AB} and a low value of $N_O^s D_O$.

It is generally believed that the provision of a greater number of short-circuit diffusion paths tends to increase D_{AB} more than D_O. Therefore, the critical concentration for protective oxide formation can be effectively decreased by reducing the alloy grain size[20–22] or increasing the dislocation density at the alloy surface by mechanical deformation via abrasion, sand blasting, shot peening, etc.[23] A higher density of defects at the alloy surface may also promote the preferential nucleation and establishment of the protective BO scale during the transient stage of oxidation.[12,24]

Selecting Alloying Additions to Promote Protective Oxide Formation

Ternary and higher order alloying additions that cause the solubility for oxygen in the alloy to decrease should, in turn, cause $N_B^o{}^*$ to decrease and, therefore, favor protective scale formation. This effect is difficult to isolate due to the potential influence of other contributing factors, but it has been invoked as a possible explanation for the beneficial effect of 2 wt.% silicon and 1 wt.% titanium additions in promoting Al_2O_3 scale formation on NiCrAlY-based alloys.[25] It is worth noting that adding elements with a high electron-to-atom ratio (e/a) can often reduce oxygen solubility.[26] This approach was adopted in a qualitative manner by Perkins et al.[27,28] in a development effort devoted to producing oxidation-resistant niobium- and titanium-aluminide alloys. However, to the authors' knowledge, there have not been any systematic studies on the dependence of $N_B^o{}^*$ on e/a.

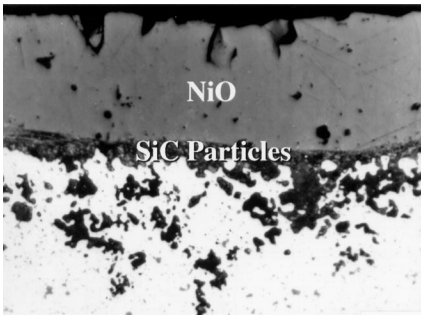

10 µm

Figure 5. A scanning electron microscopy (secondary mode) cross-section micrograph of Ni-9SiC after approximately 1 week at 1,000°C in dry air.[57]

In some cases, the critical concentration for protective scale formation can be decreased by additions of elements that form an oxide of intermediate thermodynamic stability to AO and BO. For instance, it is well known that a lower aluminum content is needed to establish and maintain an Al_2O_3 scale on M-Cr-Al alloys (where M = nickel, cobalt, or iron) than on M-Al alloys.[29] This phenomenon is generally referred to as the third-element effect. Such an effect can be extremely important from an alloy-design viewpoint, as large additions of aluminum, for example, tend to depress the melting point and increase brittleness.

The classical hypothesis for the third-element effect is based on secondary gettering, a phenomenon first proposed by Wagner[30] to explain the promotion of Al_2O_3 scale formation by zinc additions to Cu-Al alloys and chromium additions to Fe-Al alloys. According to the hypothesis, the oxide of the ternary addition develops extensively in the transient scale and thereby reduces the oxygen potential at the alloy/scale interface (i.e., N_O^s) to a value that is significantly lower than if there were no ternary addition. The lowered oxygen potential reduces the inward flux of oxygen into the alloy and consequently enables B to diffuse to the surface from the bulk without precipitating as an internal oxide, thus resulting in the development of a continuous BO scale layer at lower B concentration than in the corresponding binary alloy.

Although secondary gettering is a well-established mechanism for explaining the third-element effect, not all ternary additions that form oxides of intermediate stability have the desired effect.[31] For instance, the addition of manganese to Fe-Al alloys does not facilitate the establishment of an Al_2O_3 scale when present in high concentrations even though the stability of MnO is intermediate to FeO and Al_2O_3.[31–33] In this case, the manganese stabilizes the austenite (γ) phase, which is hypothesized to sufficiently lower aluminum diffusivity relative to that in the α-Fe(Al) phase that the third-element effect is nullified (work of Jackson and Wallwork reported in Stott et al. review article[31]). Alternative mechanisms to explain the third-element effect based, for example, on modification of subsurface diffusion behavior[34,35] have been proposed, reflecting the fact that there is not a complete understanding of how a third element may influence the formation of a protective scale on a single-phase alloy.[31]

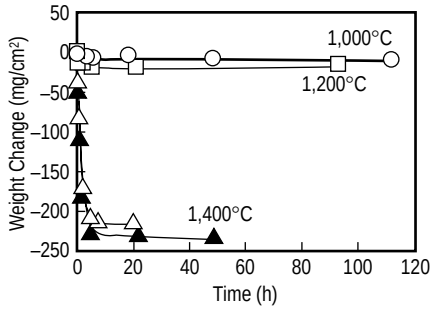

a

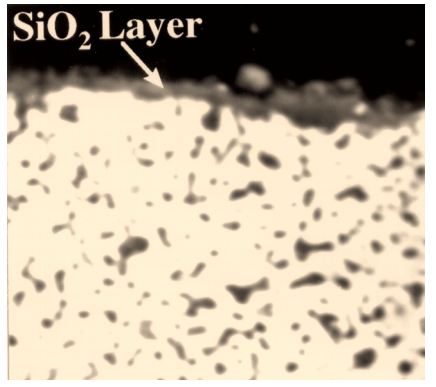

b

3 µm

Figure 6. (a) Oxidation kinetics (each data point represents a thermal cycle to room temperature) and (b) a scanning electron microscopy cross section of Mo-15Si_3N_4-6Si after 111 hours at 1,000°C in air.[57,59]

The Effect of Oxygen Partial Pressure

The critical concentration of B for protective oxide-scale formation, $N_B^o{}^*$, decreases with decreasing oxygen partial pressure since, in accordance with Sieverts's law, N_O^s decreases.[36] Thus, an increase in the oxidant pressure in a given environment may cause a borderline alloy to have a subcritical B content and exhibit nonprotective behavior. Therefore, for example, an alloy which exhibits protective scale formation at reduced oxygen partial pressures may not exhibit protective oxidation behavior in pure oxygen or air. For such alloys, pretreatment in a low oxygen partial pressure environment would favor exclusive BO scale formation. However, such pretreatments are often not practical as the protective BO scale cannot be reformed during service in the higher oxidation pressure environment if oxide-scale damage or spallation occurs.

OXIDATION OF TWO-PHASE ALLOYS

Many current alloys designed for high-temperature use are multiphase, reflecting the need to balance many needed, but often opposing properties, such as high-temperature strength and room-

temperature toughness. It is, therefore, somewhat surprising that, until recently, there has been only a limited number of studies devoted to gaining a theoretical or experimental understanding of the oxidation behavior of multiphase alloys from the viewpoint of elucidating the role of the individual phases.[37–44]

From a thermodynamic standpoint, it is worth noting that there is no distinction between the chemical stability of an element in a single-phase alloy versus a multiphase alloy. This is because equilibrium considerations require that the chemical activity of any given component must be the same in all phases of a multiphase alloy, regardless of how large the concentration difference may be. Therefore, it is the availability of the protective oxide-forming component element (i.e., chromium, aluminum, or silicon) in the multiphase microstructure that is of paramount importance, not its activity per se. Key factors include the size, shape, distribution, volume fraction, and composition of the minority phase(s), as well as the composition of the matrix phase. In general, protective scale formation is favored by small,[40] finely distributed second-phase particles.

Quantitative theoretical treatments of multiphase alloy oxidation are currently limited to two-phase, binary alloy oxidation and have focused on the kinetics and modes of internal oxidation, together with the transition from internal to external BO formation.[45–47] It has been found that, under the same oxidizing conditions, a higher concentration of B is required in a binary, two-phase alloy for protective BO scale formation than in a corresponding binary, single-phase alloy. This difference in critical concentration is predicted to increase with decreasing solubility of B in the A-rich matrix. Unfortunately, extension of these treatments to ternary and higher-order systems is not yet possible due the inclusion of numerous additional variables, related in part to the extra degree(s) of thermodynamic freedom gained. Indeed, as will be shown in a subsequent section, ternary, two-phase alloys can exhibit protective BO scale formation at a lower concentration of B than the corresponding binary AB alloy.

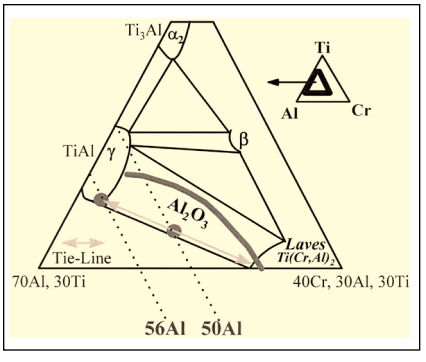

Figure 7. Schematic 1,000°C Ti-Al-Cr phase diagram[43,62,63] showing Al_2O_3-forming composition range mapped out by Perkins and Meier.[61]

From the alloy-design standpoint, it can be inferred intuitively that anything that improves the oxidation behavior of the matrix phase would aid in facilitating protective BO scale formation on a multiphase alloy. Thus, the strategies used for single-phase alloy oxidation can also be applied to two-phase alloys, including the addition of ternary or higher order elements to reduce oxygen solubility or to promote secondary gettering, as well as reducing the alloy grain size and increasing the dislocation density at the alloy surface.

The Reservoir Effect

Ternary and higher order two-phase alloys may exhibit oxidation behavior less protective than their individual component phases; between that of their component phases; and, in some rare cases, synergistically better than their component phases.[37,41] Oxidation behavior worse than their individual phases generally occurs when the phases oxidize independently of each other (Figure 3a).[41] To achieve oxidation behavior equal to or greater than that of their individual phases, the component phases in a multiphase alloy must collaborate in some manner during oxidation. The classic example is when a solute-rich second phase acts as a reservoir for the continued exclusive growth of the protective oxide scale (Figure 3b). This results in the development of a subsurface zone depleted of the solute-rich second phase, as is observed, for example, during oxidation of γ'-$Ni_3(Al,Ti)$ precipitate-strengthened nickel-based superalloys[48] and chromium-carbide dispersion-strengthened iron- and cobalt-based alloys.[49–52] A diffusional analysis to predict the depth of such subsurface zones was recently presented by Carter et al.[53]

Alloy microstructure can be critical to achieving a reservoir effect. For example, as shown in Figure 4a, a nonprotective, iron-rich oxide scale formed on as-cast Fe-15Cr-0.5C during exposure at 850°C in oxygen.[50] The alloy consisted of a γ-Fe matrix containing coarsely distributed, interdendritic chromium-rich carbides of 3 μm average size. The chromium concentration in the γ-Fe matrix was 11.2 wt.%, which is borderline for Cr_2O_3 scale formation on an Fe-Cr alloy. Hot forging the Fe-15Cr-0.5C alloy at 1,150°C caused the carbide phase to be more uniformly distributed and the carbide size to decrease to about 1 μm. The hot-forged alloy oxidized to form a thin, protective Cr_2O_3 scale under the same conditions where the as-cast material formed a nonprotective, iron-rich oxide scale (Figure 4a and 4b). A subsurface, carbide-depletion zone was present underneath the Cr_2O_3 scale on the hot-forged alloy due to the dissolution of the chromium-rich carbides to supply chromium for the growing scale.

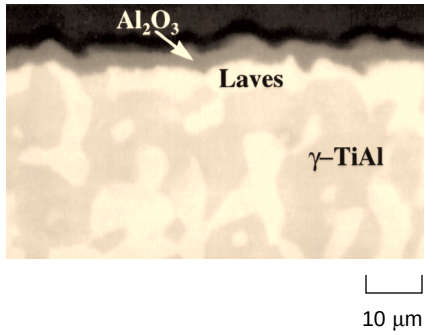

Figure 8. A scanning electron microscopy (backscatter mode) cross-section micrograph of Ti-50Al-15Cr (in at.%) after 100 h at 1,000°C in air.[63]

The matrix phase composition is also critical to promoting protective oxide-scale formation in a multiphase alloy via the reservoir effect. For example, it is well established that silicon can be beneficial in facilitating Cr_2O_3 scale formation (e.g., Reference 54), although the exact mechanism is not known.[24] Using the software package *Thermo-Calc*[55] to provide guidance, the alloy was modified to a composition of Fe-14Cr-0.4C-1Si-1Ni. The silicon partitioned primarily to the γ-Fe matrix and, further, increased the chromium concentration in the matrix from 11.2 wt.% to 12 wt.%. (Nickel was added to this alloy to stabilize the austenite phase in order to counteract the ferrite-stabilizing effect of silicon). As-cast Fe-14Cr-0.4C-1Si-1Ni oxidized to form a thin, protective Cr_2O_3 scale, supported by a chromium-carbide depletion zone (Figure 4c) similar to that observed for hot-forged Fe-15Cr-0.5C (Figure 4b).

DESIGNING TWO-PHASE ALLOYS TO INCORPORATE RESERVOIR-TYPE EFFECTS

The observation of the reservoir-effect phenomenon during the oxidation of some two-phase alloys suggests design strategies whereby two-phase microstructures are intentionally created in order to promote protective oxide-scale formation. A formal framework for such an approach does not yet exist. Indeed, a broad definition for what phenomena constitute a reservoir effect, beyond the classical example of solute-rich, second-phase dissolution in support of a growing protective oxide scale (Figure 3b), is yet to be established. However, instances of improved oxidation behavior via two-phase microstructures are beginning to emerge from the literature. Some general characteristics that lead to the promotion of protective oxide-scale formation via introduction of a second phase have been identified and can be used to provide a basis for insight into the design of new oxidation-resis-

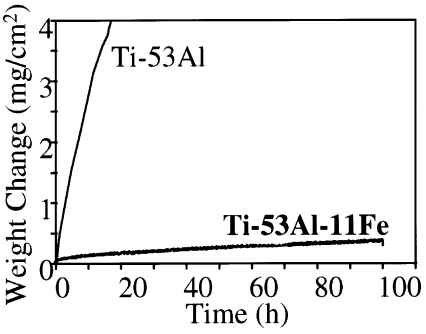

a

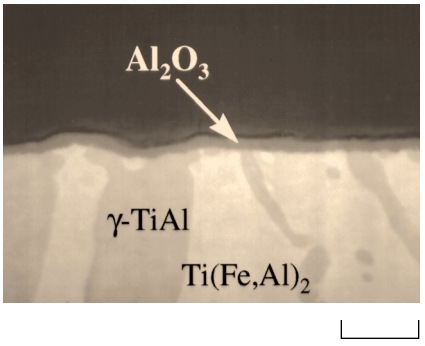

b

Figure 9. (a) Oxidation kinetics and (b) a scanning electron microscopy (backscatter mode) cross-section micrograph for Ti-53Al-11Fe (in at.%) after 100 h at 1,000°C in air.[68] In addition to γ-TiAl and $Ti(Fe,Al)_2$ (identification based solely on composition data), a minor volume fraction of the $TiAl_2$ phase may also have been present.

tant alloys. In general, they fall into one of two categories: direct addition of a second-phase compound and alloying to produce a second phase.

Compound Additions

A natural extension of the observation that second-phase chromium-rich carbide particles can act as a chromium reservoir to promote protective Cr_2O_3 scale formation[49] is the direct addition of a compound to a base alloy to induce protective scale formation.[56] This is the basis for the dispersed reservoir (DR) approach, which offers the potential to employ an alloy optimized for properties other than high-temperature oxidation resistance (e.g., toughness in a structural alloy or substrate compatibility in a coating). The DR phase should be in thermodynamic (or at least metastable) equilibrium with the matrix alloy, able to form a protective oxide more stable than the oxides of the matrix alloy, and be composed of base constituent(s) that will not detrimentally interact with either the matrix alloy or the protective oxide that is formed. Key issues relate to determining the volume fraction, particle size, and particle distribution needed to promote the formation of the DR-derived protective oxide without adversely impacting the mechanical properties of the matrix alloy.

In practice, while it would be desirable for the DR phase to dissolve underneath the growing scale to supply the protective oxide forming element (i.e., a classical reservoir effect, as illustrated in Figure 3b), this has only been observed in the special case where the external oxygen partial pressure was too low for the oxide of the matrix phase to be stable.[57] The more usual behavior is that the DR phase accumulates at the alloy/scale interface to form an inner layer that initially slows the diffusion of oxygen and/or the less protective oxide-forming constituent elements of the matrix alloy and then eventually forms a complete barrier. This has been observed when either the protective constituent element of the DR phase is insoluble in the oxide of the parent matrix alloy or when the parent matrix alloy forms volatile oxide species. For example, Stringer et al.[56] produced nickel and Ni-Si alloys containing a dispersed reservoir of SiC particles by attritor milling and extrusion. Oxidation of these alloys in air at 800°C to 1,100°C resulted in the eventual formation of a continuous SiO_2-rich layer beneath a first-formed layer of NiO (Figure 5). The mode of development of this layer appeared to involve agglomeration of SiC particles as a result of formation of NiO, in which silicon and SiC have no appreciable solubility and oxidation of the individual SiC particles to form SiO_2. The rate of oxidation was much higher than that expected for the growth of a continuous SiO_2 layer but lower than that of pure nickel.

A more dramatic effect was found for Si_3N_4 dispersed Mo-6Si.[58,59] At temperatures of 1,000–1,400°C, Mo-15Si_3N_4-6Si formed a protective SiO_2 layer following a period of evaporative weight loss, presumably of MoO_3 (Figure 6). Molybdenum loss from the surface region resulted in agglomeration of the DR Si_3N_4 particles, which eventually constituted a barrier to molybdenum transport and led to essentially protective behavior by oxidation of the individual Si_3N_4 particles to form SiO_2. The initial loss due to the formation of volatile MoO_3 was relatively small at 1,000°C and 1,200°C, but at 1,400°C (–220 mg/cm²) was equivalent to a metal surface recession of approximately 0.22 mm. Obviously, there are applications where this would not be acceptable, but the potential of the DR approach to promote protective oxide-scale formation was demonstrated.

Elemental Alloying Additions to Create a Reservoir Effect

The introduction of second phases via elemental alloying additions has also been observed to promote protective oxide-scale formation. The best example of this is the addition of chromium to Ti-Al. The γ-TiAl phase is borderline relative to forming protective Al_2O_3 in pure oxygen and is essentially incapable of forming a protective Al_2O_3 scale in air, in part due to interruption of Al_2O_3 continuity by titanium-rich nitride formation at the alloy/scale interface.[60] Perkins and Meier[61] discovered that the substitution of a minimum of 8–10 at.% chromium for titanium reduced the level of aluminum needed for protective Al_2O_3 scale formation in air from 60–70 at.% aluminum to as little as 33 at.% aluminum. This chromium effect did not result from a secondary gettering mechanism, because chromium is not of intermediate thermodynamic stability between aluminum and titanium relative to oxygen, rather it is significantly more noble. Instead, the addition of sufficient chromium to γ-TiAl introduces a second phase, the $Ti(Cr,Al)_2$ Laves phase, which aided the ability to form a protective Al_2O_3 scale in air (Figure 7).[43,62,63]

During the oxidation of two-phase γ+ Laves-phase alloys in air, the γ phase acts as an aluminum reservoir, resulting in buildup of the Laves phase at the alloy/scale interface as aluminum is consumed from the alloy to form Al_2O_3 (Figure 8). The $Ti(Cr,Al)_2$ Laves phase is borderline/capable (depending upon composition) relative to the formation of protective Al_2O_3 in air. In contrast, aluminum consumption during oxidation of single-phase binary γ-TiAl alloys (of equivalent aluminum content to the γ + Laves-phase alloys) results in the formation of α_2-Ti_3Al and cubic Z/X phase (approximate composition Ti-30Al-15O at.%) at the alloy/scale interface (e.g., References 60 and 64). The α_2-Ti_3Al phase (and likely the Z/X phase) is not capable of protective Al_2O_3 scale formation in air and has been postulated to contribute to

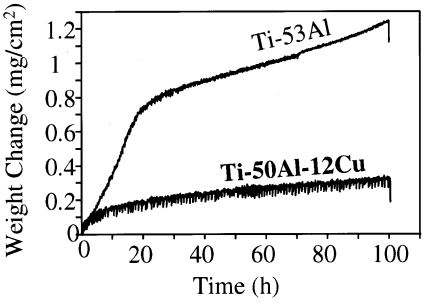

a

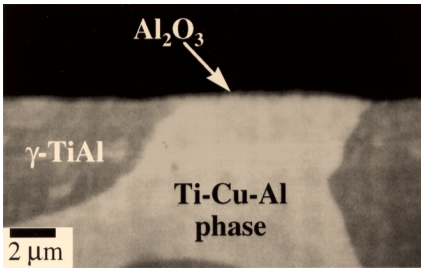

b

Figure 10. (a) Oxidation kinetics and (b) a scanning electron microscopy (backscatter mode) cross-section micrograph for Ti-50Al-12Cu (in at.%) after 100 h at 800°C in air.[69]

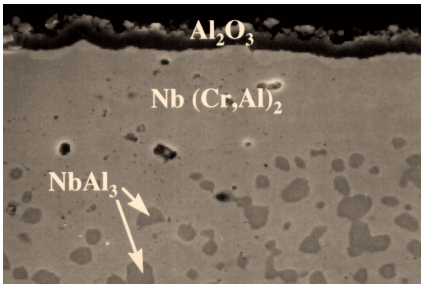

b 10 µm

Figure 11. A scanning electron microscopy (backscatter mode) cross-section micrograph of Nb-49Al-20Cr-1W-0.1Y (in at.%) after 100 one-hour cycles at 1,200°C in air.[70]

the inability to establish continuous Al_2O_3 by leading to titanium-rich nitride formation at the alloy/scale interface.[64]

Effectively, chromium acts to stabilize and sustain Laves phase at the alloy/scale interface, which allows the γ phase to act as an aluminum reservoir, rather than being depleted to form deleterious, less oxidation-resistant phases such as α_2-Ti_3Al. While a complete mechanistic understanding of protective Al_2O_3 scale formation by γ + Laves-phase Ti-Al-Cr alloys has not yet been achieved,[43,63,65–67] several unique characteristics of chromium and the Ti-Al-Cr system appear to contribute to producing this effect. First, the greater nobility of chromium in forming an oxide compared with aluminum or titanium is postulated to contribute to the tendency of the chromium-rich Laves phase to enrich at the alloy/scale during oxidation to the extent that the formation of α_2-Ti_3Al and cubic Z/X is prevented. Second, the phase fields are oriented such that, at equivalent overall aluminum content, the γ phase in a given two-phase γ + Laves-phase alloy has a much higher aluminum content (and Al/Ti activity ratio[65]) than the corresponding single-phase, binary γ-TiAl alloy.[43] For example, in Ti-50Al-15Cr (in at.%) the γ phase contains approximately 56 at.% aluminum and the Laves phase 40 at.% aluminum (Figure 7).

Based on these characteristics, a search of Ti-Al-X systems was made in order to identify element X additions that might promote protective Al_2O_3 scale formation in Ti-Al based alloys in a similar manner to chromium. Iron and copper met these criteria, and the addition of 11 at.% iron for titanium in Ti-53Al[68] (Figure 9) and the addition of 12 at.% copper for titanium in Ti-50Al[69] (Figure 10) were found to promote protective Al_2O_3 scale formation. Although these Ti-53Al-11Fe (in at.%) and Ti-50Al-12Cu (in at.%) alloys were quite brittle and did not exhibit protective Al_2O_3 scale formation over as wide a temperature/composition range as did the γ + Laves-phase Ti-Al-Cr alloys, they illustrate the potential for identifying new, oxidation-resistant alloy systems. It is interesting to note that Doychak and Hebsur[70] reported similar effects of chromium in the Nb-Al-Cr system (Figure 11), which indicates that such phenomena are not limited to Ti-Al-X systems.

CONCLUSIONS

The microstructure-based approach to multiphase alloy oxidation holds great potential for both optimizing current high-temperature structural alloys and coatings and identifying novel new oxidation-resistant alloy systems. In contrast to single-phase alloy oxidation, a quantitative, theoretical understanding of multiphase alloy oxidation is currently lacking. This is due primarily to the complexities associated with modeling multicomponent, multiphase alloy diffusion and the lack of sufficient fundamental thermodynamic and kinetic data. However, this lack of understanding does not preclude phenomenological-based studies of the oxidation of multiphase alloys, which, as shown in this overview, can provide some qualitative guidance for the design of more oxidation-resistant alloys. Such studies, ideally combined with development efforts devoted to improved mechanical properties, offer a promising route to the design of the next generation of high-temperature structural alloys and coatings.

ACKNOWLEDGEMENTS

The authors thank F. Dettenwanger, J.R. DiStefano, J.A. Haynes, C.T. Liu, J.L. Smialek, and P.F. Tortorelli for helpful comments on the manuscript. The submitted manuscript has been authored in part by contractors of the U.S. government (M.P.B., I.G.W.) under contract no. DE-AC05-96OR22464.

References

1. P. Kofstad, *High Temperature Corrosion* (London: Elsevier Applied Science Publishing, 1988), pp. 268–274.
2. E.J. Opila and N.S. Jacobson, *Fundamental Aspects of High Temperature Corrosion*, ed. D.A. Shores, R.A. Rapp, and P.Y. Hou (Pennington, NJ: Electrochemical Society, 1997), pp. 269–280.
3. M.P. Brady et al., University of Florida, Gainesville, unpublished data (1992).
4. J.L. Smialek, in this issue.
5. G.R. Wallwork, *Rep. Prog. Phys.*, 39 (1976), pp. 401–485.
6. F.H. Stott, *Rep. Prog. Phys.*, 50 (1987), pp. 861–913.
7. G.C. Wood and F.H. Stott, *Mater. Sci. Technol.*, 3 (1987), pp. 519–530.
8. D.P. Whittle, *High Temperature Corrosion*, ed. R.A. Rapp (Houston, TX: National Association of Corrosion Engineers, 1981), pp. 171–183.
9. F. Gesmundo, *Mater. Sci. Forum*, 251–254 (1997), pp. 3–18.
10. F. Gesmundo and Y. Niu, *Oxid. Met.*, 50 (1998), pp. 1–26.
11. R.A. Rapp, *Corrosion*, 21 (1965), pp. 382–401.
12. F.H. Stott, *Mater. Character.*, 28 (1992), pp. 311–325.
13. F.H. Stott and G.C. Wood, *Mater. Sci. Technol.*, 4 (1988), pp. 1072–1078.
14. D.R.G. Mitchell, D.J. Young, and W. Kleeman, *Mater. Corros.*, 49 (1998), pp. 231–236.
15. I.C. Chen and D.L. Douglass, *Oxid. Met.*, 52 (1999), pp. 195–207.
16. D.P. Whittle et al., *Acta Metall.*, 15 (1967), pp. 1747–1755.
17. C. Wagner, *Z. Elektrochem.*, 63 (1959), pp. 772–790.
18. F. Gesmundo and F. Viani, *Oxid. Met.*, 25 (1986), pp. 269–282.
19. R.A. Rapp, *Acta Metall.*, 9 (1961), pp. 730–741.
20. C.S. Giggins and F.S. Pettit, *Trans. Met. Soc. AIME*, 245 (1969), pp. 2495–2507.
21. B.A. Pint, J. Leibowitz, and J.H. DeVan, *Oxid. Met.*, 51 (1999), pp. 181–197.
22. M.S. Seltzer and B.A. Wilcox, *Met. Trans.*, 3 (1972), pp. 2357–2359.
23. D. Caplan, *Corros. Sci.*, 6 (1966), pp. 509–515.
24. B. Gleeson, to be published in *Corrosion and Environmental Degradation of Materials: Volume 19 of the Series Materials Science and Technology*, ed. M. Schütze (Weinheim, Germany: Wiley-VCH).
25. D. Clemens, W.J. Quadakkers, and L. Singheiser, *High Temperature Corrosion and Materials Chemistry*, vol. 98-9, ed. P.Y. Hou et al. (Pennington, NJ: Electrochemical Society, 1998), pp. 134–145.
26. R.T. Bryant, *J. Less Common Metals*, 4 (1962), pp. 62–68.
27. R.A. Perkins, K.T. Chiang, and G.H. Meier, *Scripta Met.*, 21 (1987), pp. 1505–1510.
28. R.A. Perkins, K.T. Chiang, and G.H. Meier, *Scripta Met.*, 22 (1988), pp. 419–423.
29. I.G. Wright, *Oxidation of Iron-, Nickel-, and Cobalt-Base Alloys*, Metals and Ceramics Information Center Report MCIC-72-07 (Columbus, OH: Battelle Columbus Laboratories, 1972).
30. C. Wagner, *Corros. Sci.*, 5 (1965), pp. 751–764.
31. F.H. Stott, G.C. Wood, and J. Stringer, *Oxid. Met.*, 44 (1995), pp. 113–145.
32. J.P. Sauer, R.A. Rapp, and J.P. Hirth, *Oxid. Met.*, 18 (1982), pp. 285–294.
33. P.R.S. Jackson and G.R. Wallwork, *Oxid. Met.*, 21 (1984), pp. 135–170.
34. S.W. Guan and W.W. Smeltzer, *Oxid. Met.*, 42 (1994), pp. 375–391.
35. W.C. Hagel, *Corros.*, 21 (1965), pp. 316–326.
36 Y.K. Rao, *Stoichiometry and Thermodynamics of Metallurgical Processes* (Cambridge, U.K.: Cambridge University Press, 1985), pp. 437–438.
37. J. Stringer, P.S. Corkish, and D.P. Whittle, *Stress Effects and Oxidation of Metals*, ed. J.V. Cathcart (New York: Met. Soc. AIME, 1975), pp. 75–93.
38. B.D. Bastow, G.C. Wood, and D.P. Whittle, *Oxid. Met.*, 16 (1981), pp. 1–32.
39. G. Wahl, *Thin Solid Films*, 107 (1983), pp. 417–426.
40. Ge Wang, B. Gleeson, and D.L. Douglass, *Oxid. Met.*, 35 (1991), pp. 333–348.
41. F. Gesmundo and B. Gleeson, *Oxid. Met.*, 44 (1995), pp. 211–238.
42. H.J. Grabke, M. Brumm, and M. Steinhorst, *Mater. Sci. Tech.*, 8 (1992), pp. 339–344.
43. M.P. Brady et al., *Acta Mater.*, 45 (1997), pp. 2371–2382.
44. M.P. Brady, E.D. Verink, Jr., and J.W. Smith, *Oxid Met.*, 51 (1999), pp. 539–556.
45. F. Gesmundo et al., *Oxid. Met.*, 42 (1994), pp. 465–484.
46. F. Gesmundo, F. Viani, and Y. Niu, *Oxid. Met.*, 42 (1994), pp. 409429.
47. F. Gesmundo, F. Viani, and Y. Niu, *Oxid. Met.*, 45 (1996), pp. 51–76.
48. M. Levy, P. Farrell, and F. Pettit, *Corros.*, 42 (1986), pp. 708–717.
49. M. E. El-Dahshan, J. Stringer, and D.P. Whittle, *Cobalt*, 4 (1974), p. 86.
50. R.N. Durham, B. Gleeson, and D.J. Young, *Oxid. Met.*, 50 (1998), pp. 139–165.
51. R. Petkovic-Luton and T.A. Ramanarayanan, *Oxid. Met.*, 34 (1990), pp. 381–400.
52. R.N. Durham, B. Gleeson, and D.J. Young, *Mater. Corros.*, 49 (1999), pp. 855–863.
53. P. Carter, B. Gleeson, and D.J. Young, *Acta Metall.*, 44 (1996), pp. 4033–4038.
54. M.J. Bennett, J.A. Desport, and P.A. Labun, *Proc. Roy. Soc. A*, 412 (1987), p. 223.
55. B. Sundman, B. Jansson, and J.O. Anderson, *CALPHAD*, 9 (1985), pp. 153–190.
56. J. Stringer et al., *Proc. 8th Intl. Congress on Metallic Corrosion* (Frankfurt am Main, Germany: DeChema, 1981), p. 655.
57. I. G. Wright, V. Nagarajan, and J. Stringer, *Corr. Sci.*, 35 (1993), pp. 841–854.
58. V. Nagarajan and I. G. Wright, "Refractory Metal Alloys Having Inherent High-Temperature Oxidation Protection," U.S. patent 4,762,557 (1988).
59. I. G. Wright and V. Nagarajan, *J. Physique IV*, C9, 3 (1993), pp. 151–157.
60. F. Dettenwanger et al., *Oxid. Met.*, 50 (1998), pp. 269–307.
61. R.A. Perkins and G.H. Meier, *Industry-University Advanced Materials Conference II*, ed. F.W. Smith (Denver, CO: Advanced Materials Institute, 1989), pp. 92–99.
62. M.P. Brady, J.L. Smialek, and F. Terepka, *Scripta Met.*, 32 (1995), pp. 1659–1664.
63. M.P. Brady et al., *Acta Mater.*, 45 (1997), pp. 2357–2369.
64. C. Lang and M. Schütze, *Mat. Corr.*, 48 (1997), pp. 13–22.
65. N.S. Jacobson, M.P. Brady, and G.M. Mehrotra, *Oxid. Met.*, 52 (1999), pp. 537–556.
66. D.A. Berztiss, F.S. Pettit, and G.H. Meier, *High Temperature Ordered Intermetallics VI*, ed. H.J. Baker et al. (Pittsburgh, PA: MRS, 1995), pp. 1285–1290.
67. F. Wang, Z. Tang, and Z.W. Wu, *Oxid. Met.*, 48 (1997), pp. 381–390
68. M.P. Brady, J.L. Smialek, and W.J. Brindley, "Oxidation-Resistant Ti-Al-Fe Alloy Diffusion Barrier Coatings," U.S. patent 5,776,617 (7 July 1998).
69 M.P. Brady, J.L. Smialek, and W.J. Brindley, unpublished research, NASA Lewis Research Center, Cleveland, OH (1997).
70. J. Doychak and M.G. Hebsur, *Oxid. Met.*, 36 (1991), pp. 113–141.

M.P. Brady and I.G. Wright are with the Metals and Ceramics Division, Oak Ridge National Laboratory. B. Gleeson is with the Department of Materials Science and Engineering, Iowa State University.

For more information, contact M.P. Brady, Metals and Ceramics Division, Oak Ridge National Laboratory, Oak Ridge, Tennessee 37831-6115; (423) 574-5153; fax (423) 574-7659; e-mail bradymp@ornl.gov.